YU ISSN 0015—3206
FZKAAA 22 (3) 529 (1990)

TESTING OF FLOW FIELD AROUND THE NOZZLE EDGE USING THE METHOD OF HOLOGRAPHIC INTERFEROMETRY

SLAVICA RISTIĆ

Vazduhoplovnotehnički institut Žarkovo, ul. Niška bb, 11132 Žarkovo, Yugoslavia

Received 10 January 1990

UDC 533.6.01

Original scientific paper

Supersonic flow around nozzle edge in wind tunnel was tested using the holographic interferometry. $M_\infty = 1.56$ was the Mach number of undisturbed flow. The nozzle edge was performed under the angle of 90 degrees. Apart the flow field visualization, the accurate flow speed determination in the region of Prandl-Mayer expansion was made possible by holographic interferogram. Theoretical and experimental results show very good agreement. The comparative advantages of holographic method relative to classical method of complex flow fields testing were considered.

1. Introduction

Holographic interferometry represents an optical method that makes possible complete flow fields testing. The method is non-contact and it does not disturb flow field. It is used for testing of flows of very large speed ranges.

The basis of this method are: holography, developed in last thirty years as the method through which the three-dimensional object image is achieved, and classic interferometry.

Very large literature exists on holography and holographic interferometry[1-6]. Its application in aerodynamic testing goes back some fifteen years ago. Today, this method is used in all known testing centres that perform flow field testing.

Air flow around aerodynamical models is very complex phenomenon. In optical sense, fluid flow field is a transparent environment with complex light refraction index spacing. Light beam, passing through such an environment,

suffers changes in its phase, so that, the information on it is carried as phase modulation. Light refraction index in each flow field point is the function of air density in that point, which, on the other side, is the function of speed, pressure and air temperature.

If, using the optical method, light refraction index arrangement in flow field is determined, all other physical parameters of tested environment, that are of significance to aerodynamic testing, can be indirectly determined as well.

Processing of interferometric image is very (sophisticated) complex process. Digitalised interferograms processing computers are used for that purpose. Interferogram two dimensional flow field testing is the simpliest case. The field created when the air flows is turned away at the nozzle edge in wind tunnel test section is chosen as an example. Holographic interferogram is recorded using two exposition.

Flow field is presented by reconstructed hologram image and it allows determination of values of different parameters in each point of tested flow.

2. *Holographic interferometry*

As it has been known, the holography represents two-stage method that, apart to light amplitude, records its phase as well. The image recording is performed in first stage, while its reconstruction is performed in the second stage. Lasers, emitting severe monochromatic, time and space coherent light beam, are used as light source.

If on the same plate the image of one object is recorded two times in different moments, in the process of reconstruction both images (figures) appear simultaneously and on the same place in space. Since the object waves are mutualy coherent (they originate from the same light beam that illuminate the hologram) they interferate and the inerference effects can be observed in the reconstructed object image. If no change occurs on object between first and second exposition, then there is no difference in images and there are no interference fringes. If certain difference appears then the reconstructed image contains the system of interference fringes that indicate that change.

If $U_{p1}(xy)$ and $U_{p2}(xy)$ are object beams during first and second exposition, and U_R is a reference beam, then using the reconstruction beam (which is the same as U_R reference beam) the reference interference beams are recuperated. Light intensity distribution in image obtained is $I(x, y)$.

$$\begin{aligned} U_{p1}(xy) &= A_1(xy) \exp \mathrm{i}(\omega t + \varphi_1(xy)) \\ U_{p2}(xy) &= A_2(xy) \exp \mathrm{i}(\omega t + \varphi_2(xy)) \\ U_R(xy) &= A_R \exp \mathrm{i}(\omega t - \alpha x) \end{aligned} \tag{1}$$

x, y are the coordinates in image plane parallel to hologram plane, while the z coordinate is in the direction of light beam movement. (A_l) amplitudes and (φ_l) phases of the reference beams are the functiones of xy coordinates. Reference, that is, reconstructive beam has constant amplitude A_R and known phase distribution.

Light intensity distribution in holographic image plane could be presented with the following approximative formula:

$$I(xy) = |U_{p1} + U_{p2}|^2 = 2\{1 + \cos[\varphi_2(xy) - \varphi_1(xy)]\} \tag{2}$$

Factors describing light wave time dependence were deleted, while the amplitudes were standardised to unit. The interference lines pattern within the image was conditioned by $\Delta\varphi(xy)$ phase difference, as seen in (2) above.

$$\Delta\varphi(xy) = \varphi_2(xy) - \varphi_1(xy) \tag{3}$$

Phase difference between two points in image can be determined if there exists the reference point where all parameters are known and if, relative to it, the interference lines up to specific point can be counted.

From the interferometry is known that light interference fringes appear if

$$\Delta\varphi(xy) = N(xy) \cdot \lambda \qquad N = 0, 1, 2, \ldots \tag{4}$$

and dark ones for:

$$\Delta\varphi(xy) = 2(N(xy) + 1) \cdot \lambda \qquad N = 0, 1, 2, \ldots \tag{5}$$

λ is light wave length, and $N(xy)$ is the number of interference fringes from reference to observed point.

Gladstone-Dale equation is the basic relation connecting flow field optical and other physical characteristics:

$$n - 1 = k \cdot \varrho \tag{6}$$

n — light refraction index

ϱ — air density

k — constant having the value of $2.25\,10^{-4}$ m^3/kg for chosen wavelength

$\Delta\varphi(xy)$ phase difference depends on light refraction index distribution. For two-dimensional fields it will be:

$$\Delta\varphi(xy) = [n_2(xy) - n_1(xy)] \cdot L \tag{7}$$

where L is path length (wind tunnel test section width) on which the light suffers changes in flow field.

If Eqs. (7), (6) are combined with (4) respectively, the result is

$$\varrho_2(xy) - \varrho_1(xy) = \frac{N(xy) \cdot \lambda}{kL} \tag{8}$$

i. e. if ϱ_∞ — is known density in undisturbed flow, then the density ϱ in any field station will be:

$$\varrho(xy) = \varrho_\infty \pm \frac{N(xy) \cdot \lambda}{k L} \tag{9}$$

Sign in front of the second member in equation (9) depends on the direction changes of interference fringes i. e. whether the density is decreasing or increasing.

Air density in all flow field stations can be calculated using Eq. (9). The density is connected with others field parameters. For example, if the air isentropic flow with ϱ_0 density, P_0 pressure and T_0 temperature in steady state is tested, then in flow $\varrho(xy)$ (9) will be first determined, while

$$P(xy) = P_0 \left(\frac{\varrho(xy)}{\varrho_0} \right)^\gamma \tag{10}$$

$\gamma = C_p/C_v$ is the relation between specific heats at constant pressure and constant volume. The air temperature will be:

$$T(xy) = T_0 \left(\frac{\varrho(xy)}{\varrho_0} \right)^{\gamma-1} \tag{11}$$

and the speed

$$V(xy) = \sqrt{2C_p T_0 \left(1 - \frac{\varrho(xy)}{\varrho_0} \right)^{\gamma-1}}. \tag{12}$$

Flow Mach number in the station with (xy) coordinates will be

$$M(xy) = \sqrt{\frac{2}{\gamma - 1} \left(\frac{\varrho_0}{\varrho(xy)} \right)^{\gamma-1} - 1}. \tag{13}$$

Known the above parameters, other important values can be determined, i. e. it is possible to perform a very precise flow field testing without introduction of probes in tested points.

3. *The description of flow field around nozzle edge*

Air supersonic flow that comes to nozzle edge changes the direction of movement for the angle of the nozzle edge. Flow reversal is performed in expansion wave that is parting from the angle end and limited by Mach waves (Fig. 1). In this region expansion and flow acceleration is created. The flow is isentropic and without turbulence. It is known as Prandtl-Meyer expansion. There exists numerous literature that deals in details with this flow[7-10].

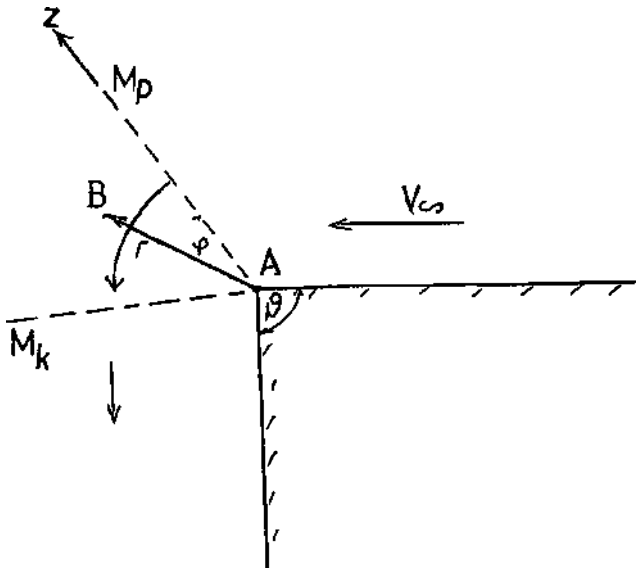

Fig. 1. Flow around the right angle edge.

In practise, flow around the supersonic nozzle edge is the phenomenon more sophisticated then the flow around insulated angle, because of the wind tunnel test section influence. This specific case is illustrated in Fig. 2, and the regions with different flow character are indicated.

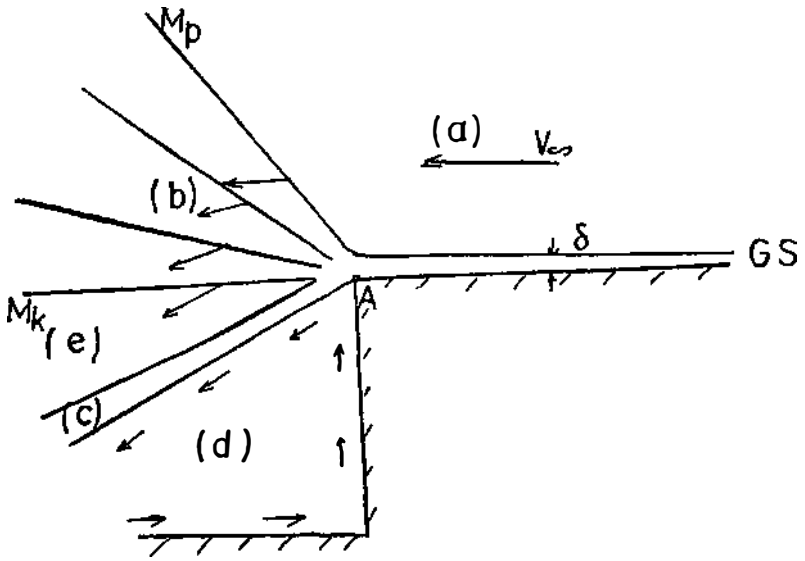

Fig. 2. Flow field around the supersonic nozzle edge in the wind tunnel.

The boundary layer of the δ thickness[11] separation occurs because of the sudden steady surface geometry change. The expansion region (b) is limited by M_p and M_k Mach waves. Behind the nozzle edge appears the region where recirculated fluid movement (d) is forming. New viscous layer where occurs the mixing of the fluid between external flow (e) that is supersonic and recirculated flow (d), that is subsonic, is formed immediatelly behind the boundary layer separation point (A). This region (c) is the tangential interruption that gradually enlarges and grows in turbulent trace. In literature[10-11] is pointed out that if the boundary layer before appearance of the expansion is laminar, and if the Reynolds number is small, then the fluid mixing region (c) is laminar in its greater part.

V_∞ is flow speed in region (a), i. e. in the undisturbed flow. C_∞ is speed of sound, while C^* represents critical speed.

It is convenient to introduce cylindric coordinates to describe the flow in expansion area, in the way that z axis coincides with angle edge (with the edge of rigid surface). There are also r and φ coordinates, r represents the distance of point to z axis, while angle φ is in fact the sum of angles awarded to initial Mach wave according to Eq. (14) and of angle from certain point up to initial Mach line.

$$\varphi = \varphi_p + \varphi_B$$

$$\varphi_p = \sqrt{\frac{\gamma+1}{\gamma-1}} \arccos \frac{C}{C^*}. \tag{14}$$

Flow speed components (7) can be represented in cylindric coordinates

$$V = \sqrt{V_\varphi^2 + V_r^2}$$

$$V_\varphi = C^* \cos \sqrt{\frac{\gamma-1}{\gamma+1}} \cdot \varphi \tag{15}$$

$$V_r = \sqrt{\frac{\gamma+1}{\gamma-1}}\, C^* \sin \sqrt{\frac{\gamma-1}{\gamma+1}} \cdot \varphi$$

and Mach number will be:

$$M = V/V_\varphi \tag{16}$$

since $V_\varphi = C$.

Mach wave angle relative to flow direction is

$$\alpha_M = \arcsin \frac{1}{M}. \tag{17}$$

Since the field is two-dimensional, there is no change of flow field parameters along z axis. Dependence on r is very small and could be neglected. All magnitu-

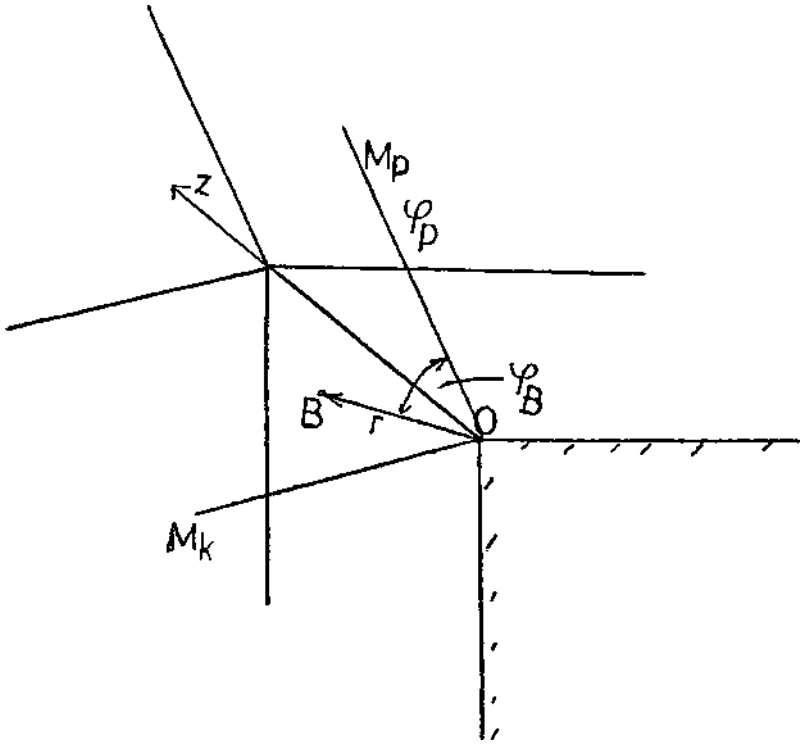

Fig. 3. Description of cylindric coordinate system.

des near the nozzle edge are significantly depending on (14) coordinate. This coordinate has certain initial value that is depending on relation of speed of sound and critical speed C^*

$$C^* = \sqrt{\frac{\gamma - 1}{\gamma + 1} V_\infty^2 + \frac{\gamma + 1}{2} C_\infty^2}\,. \tag{18}$$

ψ angle, that forms speed vector with a certain given direction, is:

$$\psi = \varphi + \operatorname{arctg} \frac{V_\varphi}{V_r}. \tag{19}$$

V_φ component is normal on r vector radius and in each point it is equal to c local speed of sound magnitude (16). Sets of points on line $\varphi = \text{const}$, are of the same value as the flow field parameters.

Line $\varphi = \text{const.}$ is intersected by streamlines under perturbance angle $\beta = \sin \frac{V_\infty}{V} = \sin \frac{C}{V}$ i. e. these are characteristics. One family of characteristics represents beam of lines coming out from a singular point.

The analysis of physic flow parameters passing through expansion region show that

$$\frac{dp}{d\varphi} < 0 \qquad \frac{d\varrho}{d\varphi} < 0 \qquad \frac{dV}{d\varphi} > 0 \tag{20}$$

i. e., in the direction of bypassing the singular point that coincide with circulation direction, density and pressure decrease, while the speed increases.

The family of characteristic lines appearing in expansion region between M_p and M_k, represents the set of lines that connect points with the same air density i. e. with the same light refraction index. If the testing of flow field is performed with holographic interferometry method, than each line will be visualized, i. e. »seen« as one interferometric line, dark of light, in dependence of phase difference.

4. Experiment description

In order to demonstrate advantages of holographic interferometry in complex flow field testing, and compared with other classical methods, the experiment is performed in supersonic wind tunnel at flow speeds $V_\infty = 440$ m/s ($M_\infty = 1.56$).

Wind tunnel test section size is 250 mm × 250 mm with windows, enabling the usage of optical methods (Schlieren and holographic interferometry). Upper and lower nozzle plates are 250 mm wide. Flow field around nozzle edge is strictly two-dimensional. The edge is performed under the angle of 90 degrees. Records were executed also with empty wind tunnel and with the tunnel equipped with calibration cone with the angle near the top of $\vartheta_c = 30$ degrees and with diameter base $D = 26$ mm.

The usage of classical methods of nozzle edge flow field testing comprises the introduction of probe within the expansion region and holes perforation on nozzle surface. These interventions would significantly change the flow field and give the erroneous image of processes. Furthermore, it would be necessary to have very dense grating of measuring points, making this method very inefficient. In realization of this experiment (Fig. 4) the holographic interferometer was used.

As recording system light source the ruby laser (2) was used, while He-Ne (3) was used for setting. The laser light was, by means of lens and mirrors, devided in two parts, enlarged and collimated. One part U_p passed through wind tunnel test section (11) and, as object beam, fell on holographic plate (9). Other part of light beam was conducted across wind tunnel and sent to holographic plate. That is so called referent (U_R) or auxiliary light beam. Holographic plate was exposed two times: when the wind tunnel was no operating (when exists (homogeneous) flow field distribution U_{p1}) and at the moment of operation of wind tunel when there was complex flow, field that was the subject of testing. Standard plates with fine grain emulsion (8E75, AGFA GEVAERT) were used for hologram recording. Stagnation pressure (P_0), atmospheric pressure P_a and Mach number M_∞ were measured also by basic measuring system in wind tunnel.

Holographic images were reconstructed by He-Ne laser and the photos were taken. They were used for numerical calculation of flow field parameters.

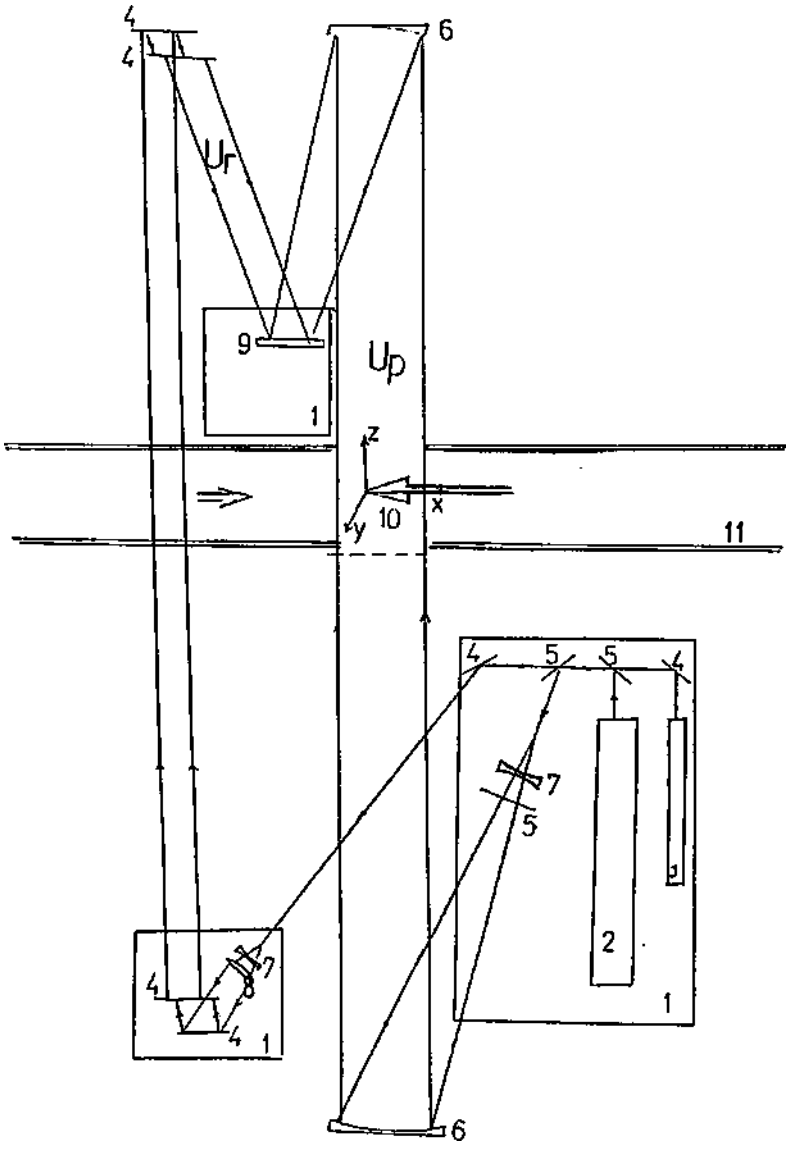

Fig. 4. Schematic diagram of the holographic interferometer.

5. *Results analysis*

The photos of holographic images taken in supersonic wind tunnel are presented on Figs. 5 and 6. First figure represents the complete test section with model, cone with $\vartheta_c = 30°$, while nozzle surface and its edges are seen on the up-

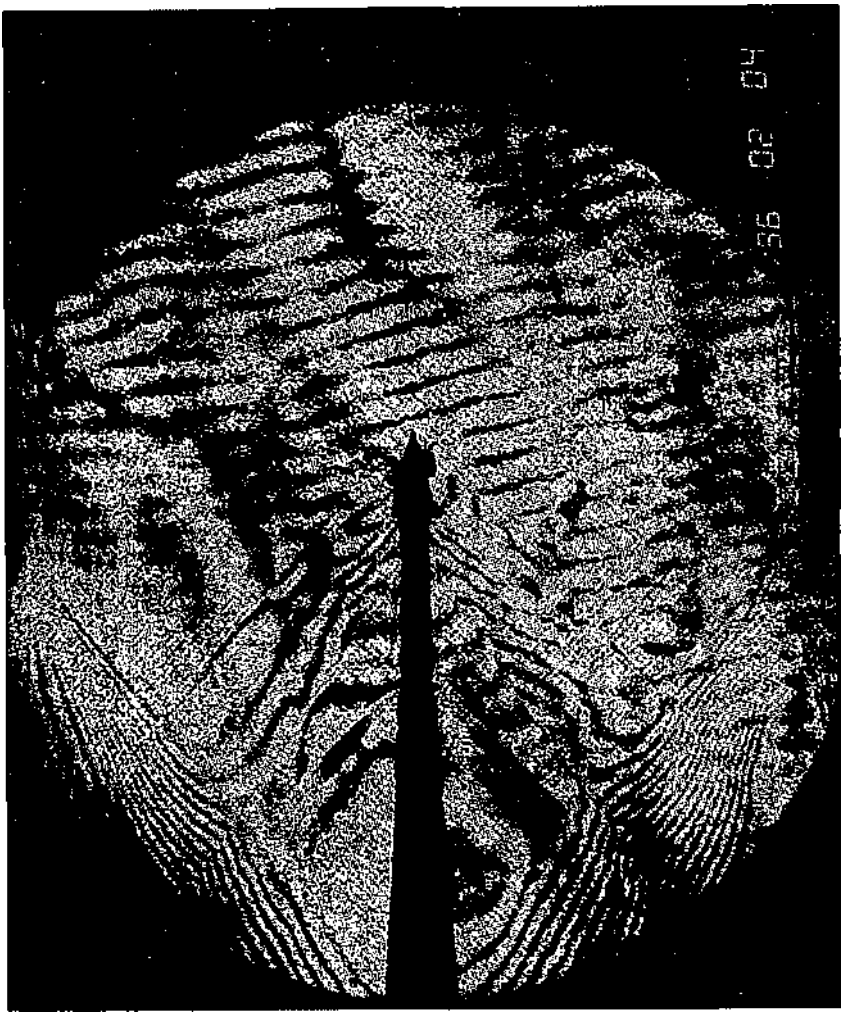

Fig. 5. Photo of holographic interferogram which represents complete test section.

per and lower part, respectively. Flow around model and at the nozzle ends is described by interference fringes.

The flow in front of the model was homogenous with constant parameters, and therefore in that part of the photo there is the system of equidistant lines representing the reference system, since the method of finite width interference fringes was used. The axisymmetric flow field was formed around the cone, behind the shock wave tied at the cone top. Boundary layers are seen in near vicinity of nozzle surface. The expansion fan is formed on the edge. It fills the region where the speed vector deflects and its apsolute value increases.

A detail of flow field in nozzle edge vicinity is presented in Fig. 6. This interferogram is used for reading out the interference fringes ordinal number (N) and

Fig. 6. Flow field interferogram in nozzle edge vicinity.

for calculation of speed values in specific points. Hologram, the image of which is presented in Fig. 6, is recorded by two-exposition method, while the interference fringes are of non-finite width. In the region above the nozzle where the flow is homogeneous, because of the laser light non-filtrated beam and parasitic effects that happen between two expositions, the image is non-homogeneous. Based on the theories presented in literature[7], flow field parameters theoretic calculations are performed. Obtained results are presented in first part of Table 1. N number is the characteristic value for each interference fringe. $N = 0$ is added to the light field (region) in front of the expansion fan. That is the point inhomogeneous flow with known flow speed, i. e. Mach number ($M_\infty = 1.56$) (9). $N = \frac{1}{2}$ belongs to the first dark fringe, i. e. to all its points. Points that form the next light line (fringe) have $N = 1$.

The last dark line in expansion region (b) has $N = 16\ 1/2$. Zone (e) is the region where exists the supersonic flow of $V_k > V_p$ speed and it is relatively homogeneous. Since the whole area can be considered as one fringe, the interference line $N = 17$ belongs to it.

TABLE 1.

N	φ (o)	χ (o)	V_φ (m/s)	V_r (m/s)	V (m/s)	M	α_M (o)	ϱ_N (kg/m^3)	$\Delta\varrho_N$ (kg/m^3)	ϱ_N/ϱ_0	V_{NF} (m/s)	M_{NF}	M_{NT}
0			283.4		442	1.56	40	0.4452	0	0.3710	433	1.56	1.56
1	64	103	284.5	334.15	449	1.565	39	0.4327	0.01245	0.3604	438	1.59	1.59
2	67	104.3	281.4	348.75	447	1.588	38.5	0.4203	0.02491	0.3503	443	1.61	1.62
3	69	106	279.6	358.7	454.8	1.627	37.5	0.4078	0.03734	0.3398	448	1.64	1.65
4	71	107.5	277.2	367.7	460.5	1.661	36.5	0.3954	0.04981	0.3295	453	1.67	1.67
5	73	108.6	275.4	376.5	466.5	1.694	36	0.3829	0.0623	0.3191	458	1.70	1.70
6	74.5	109.2	273.1	384.37	471.5	1.726	35	0.3704	0.0747	0.3087	463	1.73	1.74
7	76	110.2	272.2	390.9	476.35	1.75	34.5	0.3578	0.0872	0.2983	469	1.76	1.76
8	78	111.5	269.9	399.8	482.5	1.787	33.5	0.3455	0.0996	0.2879	474	1.80	1.80
9	80	112.6	267.5	409.4	489.05	1.828	32.8	0.3331	0.1121	0.2776	479	1.83	0.83
10	82	113.8	264.9	418.9	495.7	1.870	32	0.3210	0.1245	0.2675	484	1.86	1.87
11	84	115	262.7	427.24	501.4	1.908	31	0.3085	0.1370	0.2571	490	1.90	1.90
12	86	116.2	260.2	434.92	56.75	1.945	30.5	0.2961	0.1495	0.2467	495	1.94	1.94
13	88	117.5	257.7	445.02	514.23	1.995	29.9	0.2836	0.1619	0.2363	501	1.98	1.98
14	89	117.9	256.1	449.65	517.47	2.02	29.3	0.2712	0.1743	0.2260	507	2.02	2.02
15	90.5	118.5	253.3	455.83	521.48	2.06	28.9	0.2587	0.1868	0.2156	512	2.06	2.06
16	92	119.3	252.3	463.17	527.43	2.09	28.3	0.2463	0.1992	0.2053	518	2.10	2.10
17	94	122	250.1	470.89	533.2	2.13	27.5	0.2338	0.2117	0.1949	524	2.15	2.15

Theoretical and experimental flow field parameters obtained through equations (14) to (21) and holographic interferogram.

The mixing zone (c) that is under region (e), is mostly laminar, as expected, and can be seen on the photo. The flow under mixing zone is subsonic (d), Fig. 2. The density changes in that area are not great enough to be recorded. For visualization of this flow it is necessary to introduce additional air density gradient.

The value for the region influenced by expansion wave are presented in Table 1. The magnitudes φ, ψ, V_φ, V_r, V, M, a_M are calculated through Eqs. (14) to (21) respectively, and through values measured by wind tunnel primary measuring system.

$$T_0 = 298\ \mathrm{K}$$

$$T_\infty = 200.44\ \mathrm{K}$$

$$C_\infty = 283\ \mathrm{m/s}$$

$$C^* = 315.4\ \mathrm{m/s}.$$

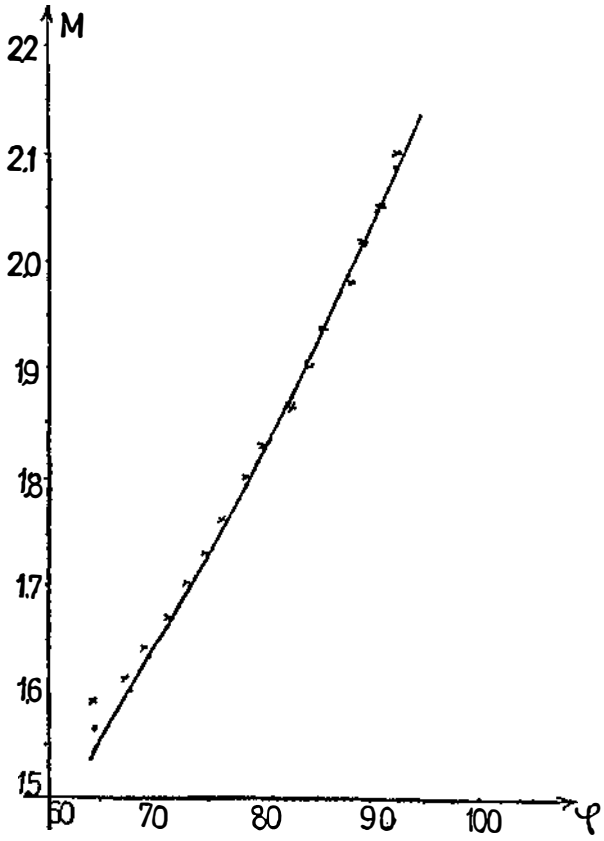

Fig. 7. Theoretical and experimental values of Mach number in the expansion area.

Flow Mach number changes from 1.56 to 2.13, while the speed changes from 442 to 533 m/s. Flow field parameters values obtained through holographic interferogram are presented in second part of Table 1. $\varrho_{\infty} = 0.4452$ kg/m^3 is air density in undisturbed flow. Air density for points laying on separate interference fringes is calculated through Eqs. (9), (11) and (12). $\varrho_0 = 1.2$ kg/m^3 density. Test section length $l = 0.25$ m, and ruby laser light wave length $\lambda = 694.3\,10^{-9}$ m. Gladston-Dale constant is $K = 2.25\,10^{-4}$ m^3/kg. Mach number M_{NF} is directly calculated through cited formulas, while M_{NT} for given pressure and ϱ_N/ϱ_0 ratio is read from tables in literature[8].

According to obtained data, Mach number is changed from 1.56 to 2.15. The dependence of M from φ for the region between initial and end Mach wave is presented on Fig. 7.

Very good agreement between M_{NF} experimental values and M_{NT} theoretic calculated values was achieved. Mean relative error was about 1%. Values obtained for M were applicable to point set laying on the same interference fringe ($N =$ = const.). The read-out performed in this testing was very rude ($N = 0.5$). Flow field analysis performed by this method can be much more accurate if the system for digitalisation and image processing in 512×512 (or 1024×1024) points with 256 shades of grey is used.

6. *Conclusion*

Testing of flow field around the nozzle edge using the method of holographic interferometry showed the basic advantages of this method, compared with the classical ones:

- Holographic interferometry is the optical method that allows complete flow field visualization.
- The method is non-contact and it doesn't disturb the flow field.
- It allows the observation of flow field characteristic regions: shock waves, expansion waves, Mach waves, boundary layer, turbulence etc.
- It allows the calculation of flow field parameter values for each point within the wind tunnel test section.
- For two-dimensional and axisymetric flow fields one interferogram is enough and for the asymmetric fields it is necessary to record three interferograms under different angles.
- The method is very economical and it is possible to obtain a great number of information from small number of experiments (i. e. for one interferogram recording one wind tunnel ran of 10 s duration is necessary).
- Generaly, there are no limitations relative to object dimensions. Everything is depending on laser power and optical components.
- Top quality optical components (lens, mirrors, windows) are not required.
- The method can be used for flow testing of different fluids, air, water, liquids and their mixtures. Sufficiently large density gradient, that can be the result of internal changes or provoked from the outside, is the basic requirement.
- The mehtod is very accurate. The degree of utilisation of given possibilities depends on processing method of holographic interferograms.

Nowadays, a great deal of research is made on developing of holographic interferograms recording techniques, elimination of parasite effects and image processing acceleration (thermoplastic films and plates). Furthermore, many researches are made in the fields of digitalisation, interferogram filtering, in the final processing of digitalised image and connecting flow field optical and aerodynamic characteristics.

References

1) C. Vest, *Holographic Interferometry* Academic Press, New York, 1983;
2) Ю. и Денисюк, Ю. И. Островский, Оптическая голография и ее примененый, Наука, Ленинград 1977;
3) J. R. Collier, C. B Burckhardt., L. H. Lin, *Optical Holography*, Academic Press, New York, 1971;
4) W. J. Jang, *Flow Visualization III*, Hemisphere publishing, New York, 1985;
5) R. D. Matulka, D. J. Collins of Appl. Phys. **42** (1971) 1109;
6) G. S. Settles, AIAA Journal **24** (1986) 8;
7) L. D. Landau, E. M. Lifšic, *Mehanika neprekidnih sredina*, Građevinska knjiga, Beograd 1965;
8) Z. Rendulić, *Aerodinamika*, 1965;
9) J. D. Anderson, AIAA Journal **15** (1983) 5;
10) J. Floyd and J. R. Wilcox, AIAA Journal **26** (1988) 3;
11) I. S. Donaldson, AIAA Journal **5** (1967) 6.

ISPITIVANJE STRUJANJA OKO RUBA MLAZNIKA POMOĆU METODE HOLOGRAFSKE INTERFEROMETRIJE

SLAVICA RISTIĆ

Vazduhoplovnotehnički institut Žarkovo, ul. Niška bb, 11132 Žarkovo

UDC 533.6.01

Originalni znanstveni rad

Nadzvučno strujanje oko ruba mlaznika u aerotunelu je ispitano pomoću holografske interferometrije. Mahov broj neporemećene struje je $M_\infty = 1.56$. Rub mlaznika je izveden pod uglom od 90°. Pored vizualizacije strujnog polja, holografski interferogram je omogućio i precizno određivanje brzine strujanja u području Prandel-Majerove ekspanzije. Teorijski i eksperimentalni rezultati pokazuju veoma dobro slaganje. Razmatrane su komparativne prednosti koje holografska metoda poseduje u odnosu na klasične metode ispitivanja složenih strujnih polja.